



# Numerical study of melting effect with entropy generation minimization in flow of carbon nanotubes

Fawaz E. Alsaadi<sup>1</sup> · Khursheed Muhammad<sup>2</sup> · T. Hayat<sup>2,3</sup> · A. Alsaedi<sup>3</sup> · S. Asghar<sup>4</sup>

Received: 31 December 2018 / Accepted: 16 August 2019 / Published online: 25 September 2019  
© Akadémiai Kiadó, Budapest, Hungary 2019

## Abstract

Optimization of entropy generation in squeezing flow of carbon nanotubes is addressed. Nanoparticles consist of single- and multiple-walled carbon nanotubes. Heat transfer subject to melting effect is employed. Shooting technique along with the fifth-order Runge–Kutta algorithm (bvp4c) is employed for the simulation. Bejan number, entropy generation rate, velocity and temperature are studied. Nusselt number and skin friction are also discussed. Velocity intensifies for higher estimations of squeezing parameter, nanoparticle volume fraction and melting parameter, while it reduces the temperature of fluid. Nusselt number enhances with an increment in estimations of squeezing parameter, nanoparticle volume fraction and melting parameter. Rate of entropy production decays with higher nanoparticle volume fraction and squeezing parameter. Bejan number is an increasing function of squeezing parameter, while it decays with an increment in melting parameter and nanoparticle volume fraction. Furthermore, prominent behavior is shown by multiple-walled CNTs.

**Keywords** Entropy generation · Bejan number · Melting effect · Carbon nanotubes (single- and multi-walled) · Squeezed flow

## List of symbols

|              |                                       |
|--------------|---------------------------------------|
| $u, v$       | Velocity components                   |
| $x, y$       | Coordinates                           |
| $\mu_f$      | Fluid dynamic viscosity               |
| $\nu_{nf}$   | Kinematic nanofluid viscosity         |
| $\rho_f$     | Fluid density                         |
| $\nu_f$      | Kinematic fluid viscosity             |
| $k_f$        | Base fluid thermal conductivity       |
| $(c_p)_f$    | Specific heat of base fluid           |
| $f', \theta$ | Dimensionless (velocity, temperature) |

|               |  |
|---------------|--|
| $\Omega$      | Non-dimensional temperature difference |
| $P_1$         | Pressure                               |
| $T$           | Temperature of nanoliquid              |
| $T_m$         | Melting surface temperature            |
| $T_h$         | Upper wall temperature                 |
| $\mu_{nf}$    | Nanofluid dynamic viscosity            |
| $S_{G_0}$     | Characteristic entropy generation      |
| $\alpha_f$    | Thermal diffusivity of base fluid      |
| $c_{pf}$      | Specific heat of base fluid            |
| $k_{nf}$      | Nanofluids thermal conductivity        |
| $(c_p)_{nf}$  | Specific heat of nanofluid             |
| $\alpha_{nf}$ | Thermal diffusivity of nanofluid       |
| $Pr$          | Prandtl number                         |
| $k_{CNT}$     | Thermal conductivity of CNTs           |
| CNTs          | Carbon nanotubes                       |
| $\phi$        | Nanoparticle volume fraction           |
| $Ec_1$        | Local Eckert number                    |
| $\tau_w$      | Shear stress                           |
| $Sq$          | Squeezing parameter                    |
| $M$           | Melting parameter                      |
| $T_0$         | Solid surface temperature              |
| $c_s$         | Solid surface heat capacity            |
| $Ec$          | Eckert number                          |

✉ Khursheed Muhammad  
kmuhammad@math.qau.edu.pk; khursheedfaiq@gmail.com  
T. Hayat  
fmgpak@gmail.com

<sup>1</sup> Department of Information Technology, Faculty of Computing and Information Technology, King Abdulaziz University, Jeddah, Saudi Arabia

<sup>2</sup> Department of Mathematics, Quaid-I-Azam University, Islamabad 44000, Pakistan

<sup>3</sup> Nonlinear Analysis and Applied Mathematics (NAAM) Research Group, Department of Mathematics, Faculty of Science, King Abdulaziz University, Jeddah, Saudi Arabia

<sup>4</sup> Department of Mathematics, CUI, Park Road Chak Shahzad, Islamabad, Pakistan

## Introduction

Nanoliquids, a novel thermo-fluids class engineered through stable adjournment of nanosized metallic/non-metallic objects (droplets, tubes, fibers, particles) in base materials with improved conductivity, exhibit the effective thermal management advantages with compactness. Nonetheless the intensification of thermal conductivity is not the main component accountable for nanofluids developed thermal efficiency, other aspects like sedimentation, gravity, inter-phase resistive force, dispersion, gravity, airborne phonon advection, invariable shear rate, migration of nanoparticles persuaded via layering and viscosity gradient at solid–liquid boundary also have a noteworthy contribution. The hydrothermal features of nanoliquids are revealed through the net impact of relative alterations in nanofluids thermophysical characteristics which are sympathetic regarding multiple factors comprising particle morphology (shape and size), pH value and base liquid characteristics, material temperature and additives. No doubt the amalgamation of disseminated solid elements in base liquid demonstrates extraordinary rise in thermophysical characteristics and maintains vast utilizations for illustration functioning of heat exchanger, thermal defiance, nuclear reactors cooling, etc. Choi [1] elaborates that nanoparticles size ought to be under 50 nm to convalesce heat transportation of ordinary materials. Later, with an innovation of technology in contemporary industry the nanoliquids with size under 100 nm have been established for distinct engineering functionalities. Various nanoliquid models (single-phase, two-phase, CNTs, Tiwari and Das) are reported to investigate nanotechnology [2–7]. Some recent works in this direction can be seen in Refs. [8–19].

Investigation regarding entropy generation and utilization of energy introduces a significant methodology in the thermal design and turns out to be the prime concern in numerous engineering demands for illustration (micro-electronics, nuclear reactors chilling, heat exchangers, boiler and solar collectors). Precision estimation regarding entropy generation elucidates energy dissipation of a system effectively and consequently is a trustworthy device to acquire an optimum design in several industries. No doubt heat transportation intimate links with the thermodynamics first relation which is the only thermodynamic principle utilized in traditional heat transportation analysis. Thermodynamics second relation delivers an amount regarding rate of entropy generation or irreversibility in a system or procedure and accordingly influences the effectiveness of heat transportation process. Recently, increasing interest about irreversibility influence on energy interactions is noted. Initial analysis about entropy generation is elaborated by Bejan [20–22]. He revealed that entropy in

convective liquid flow is owing to shear stresses and heat transportation. Numerous investigators employed entropy concept to minimize irreversibility of heat transport problems like boiling phenomenon and steam turbines [23]. Further, recent investigations covering entropy generation concept can be consulted through the Refs. [24–32].

The researchers at present have considerable concern about improvement for energy storage and heating/cooling rate in various modern and advanced technologies. In this direction, numerous flow problems have been formulated considering different kinds of distributions (wall to ambient temperature) utilizing various fluid models. Nonetheless, major problem for researchers is to introduce extraordinary storing of energy through minimal price. Some advanced technologies like waste heat retrieval, solar energy and simultaneous heat/power plants necessitate economically more apposite and effectual approach to store energy. In general, three approaches are utilized regarding energy storing, that is sensible heat, latent heat and chemical/thermal energy. Among these approaches, the latent heat is regarded more apposite and well organized (by altering the materials phase). Consequently, thermal energy in a material is stowed via latent heat through melting procedure. Melting process is extremely vital in processes comprising soil melting, the soil freezing around heat exchanger loops of a field-based pump, permafrost melting, magma solidification, frozen grounds thawing, freeze cure of sewage, semiconductor material preparation, welding and molding of an industrial process [33]. Various researches have elaborated melting aspect under different flow configurations (see Refs. [34–39]).

In this paper, we have studied entropy generation in dissipative flow of carbon nanotubes. Melting heat is accounted. Analysis is carried out between two infinite plates. Systems of differential equations are obtained via implementing suitable variables. Shooting method (bvp4c) is used for solutions development. Physical quantities are discussed.

## Formulation

Unsteady squeezed flow of carbon nanomaterial is assumed between two parallel plates. Both plates are distant  $h(t)$  apart. Lower plate (at  $y = 0$ ) is stretched with velocity  $U_w = \frac{ax}{1-ct}$ , while the plate at  $y = h(t)$  is set in motion toward the plate at  $y = 0$  with a squeezing velocity  $v_h = \frac{dh}{dt} = \sqrt{\frac{b_1(1-ct)}{a}}$ . Melting heat is considered for heat transfer. Entropy generation effect is considered. Flow is parallel to  $x$  axis, while  $y$  axis is normal to it. Expressions under interest are [11]:

$$\frac{\partial u}{\partial x} + \frac{\partial v}{\partial y} = 0, \tag{1}$$

$$\rho_{nf} \left( \frac{\partial u}{\partial t} + u \frac{\partial u}{\partial x} + v \frac{\partial u}{\partial y} \right) = - \frac{\partial p_1}{\partial x} + \mu_{nf} \left( \frac{\partial^2 u}{\partial x^2} + \frac{\partial^2 u}{\partial y^2} \right), \tag{2}$$

$$\rho_{nf} \left( \frac{\partial v}{\partial t} + u \frac{\partial v}{\partial x} + v \frac{\partial v}{\partial y} \right) = - \frac{\partial p_1}{\partial y} + \mu_{nf} \left( \frac{\partial^2 v}{\partial x^2} + \frac{\partial^2 v}{\partial y^2} \right), \tag{3}$$

$$\begin{aligned} \frac{\partial T}{\partial t} + u \frac{\partial T}{\partial x} + v \frac{\partial T}{\partial y} = \alpha_{nf} \left( \frac{\partial^2 T}{\partial x^2} + \frac{\partial^2 T}{\partial y^2} \right) \\ + \frac{\mu_{nf}}{(\rho c_p)_{nf}} \left[ 4 \left( \frac{\partial u}{\partial x} \right)^2 + \left( \frac{\partial v}{\partial x} + \frac{\partial u}{\partial y} \right)^2 \right], \end{aligned} \tag{4}$$

with boundary conditions

$$\begin{aligned} u = U_w(x) = \frac{ax}{1-ct}, \quad T = T_m \text{ at } y = 0, \quad u = 0, \\ v = v_h = \frac{dh}{dt}, \quad T = T_h \text{ at } y = h(t). \end{aligned} \tag{5}$$

Melting condition is [5]:

$$k_{nf} \left( \frac{\partial T}{\partial y} \right) = \rho_{nf} (\lambda_1 + c_s(T_m - T_0))v \text{ at } y = 0. \tag{6}$$

The expressions used in theoretical model proposed by Xue [40] are

$$\begin{aligned} \mu_{nf} = \frac{\mu_f}{(1-\phi)^{2.5}}, \quad \nu_{nf} = \frac{\mu_{nf}}{\rho_{nf}}, \quad \rho_{nf} = (1-\phi)\rho_f + \phi\rho_{CNT}, \\ \alpha_{nf} = \frac{k_{nf}}{\rho_{nf}(c_p)_{nf}}, \quad \frac{k_{nf}}{k_f} = \frac{(1-\phi) + 2\phi \frac{k_{CNT}}{k_f} \ln \frac{k_{CNT} + k_f}{k_{CNT} - k_f}}{(1-\phi) + 2\phi \frac{k_f}{k_{CNT} - k_f} \ln \frac{k_{CNT} + k_f}{2k_f}}, \end{aligned} \tag{7}$$

We use the transformations [38]:

$$\begin{aligned} \eta = \frac{y}{h(t)}, \quad u = \left( \frac{ax}{(1-ct)} \right) f'(\eta), \quad v = -\sqrt{\frac{av_f}{1-ct}} f(\eta), \\ \theta(\eta) = \frac{T - T_m}{T_f - T_m}, \end{aligned} \tag{8}$$

where

$$h(t) = \sqrt{\frac{v_f(1-ct)}{a}}. \tag{9}$$

Equation (1) is verified, while the other equations reduced to

$$\begin{aligned} \left( \frac{1}{(1-\phi)^{2.5}(1-\phi + \phi \frac{\rho_{CNT}}{\rho_f})} \right) f^{(iv)} - f'f'' + ff''' - \frac{Sq}{2}(3f'' + \eta f''') \\ = 0, \end{aligned} \tag{10}$$

$$\begin{aligned} \left( \frac{k_{nf}/k_f}{(1-\phi + \phi \frac{(\rho c_p)_{CNT}}{(\rho c_p)_f})} \right) \theta'' + Pr(f\theta' - \frac{Sq}{2}\eta\theta') \\ + \frac{Pr}{(1-\phi)^{2.5}(1-\phi + \phi \frac{(\rho c_p)_{CNT}}{(\rho c_p)_f})} (4Ec_1f'^2 + Ec_1f''^2) \\ = 0. \end{aligned} \tag{11}$$

$$\begin{aligned} f'(0) = 1, \quad \theta(0) = 0, \\ \left( \frac{k_{nf}}{k_f} \right) M\theta'(0) + Pr(1-\phi + \phi \frac{\rho_{CNT}}{\rho_f})f(0) = 0, \\ f'(1) = 0, \quad f(1) = 1, \quad \theta(1) = 1. \end{aligned} \tag{12}$$

The involved dimensionless parameters are

$$\begin{aligned} Sq = \frac{c}{a}, \quad Pr = \frac{v}{\alpha}, \quad Ec = \frac{v_f^2}{h^2(c_p)_f(T_m - T_h)}, \\ Ec_1 = \frac{U_w^2}{(c_p)_f(T_m - T_h)}, \\ M = \frac{c_{pf}(T_\infty - T_m)}{\lambda + c_s(T_m - T_0)}, \quad \eta = \frac{y}{h(t)}. \end{aligned} \tag{13}$$

### Expressions of skin friction coefficient ( $C_f\sqrt{Re_x}$ ) and Nusselt number ( $\frac{Nu_x}{\sqrt{Re_x}}$ )

Expressions for  $C_f\sqrt{Re_x}$  and ( $\frac{Nu_x}{\sqrt{Re_x}}$ ) in dimensional and non-dimensional forms are [11]:

$$C_f = \frac{(\tau_{xy})_{y=0}}{\rho_f U_w^2}, \quad Nu_x = \frac{xq_w}{k_{nf}(T_f - T_h)}, \tag{14}$$

where

$$\tau_{xy} = \mu_{nf} \left( \frac{\partial u}{\partial y} \right)_{y=0}, \quad q_w = -k_{nf} \left( \frac{\partial T}{\partial y} \right)_{y=0} \tag{15}$$

$$\begin{aligned} \text{or } C_f\sqrt{Re_x} = \frac{1}{(1-\phi_1)^{2.5}(1-\phi_2)^{2.5}} f''(0), \\ \frac{Nu_x}{\sqrt{Re_x}} = -\frac{k_{nf}}{k_f} \theta'(0), \end{aligned} \tag{16}$$

where  $Re_x = \sqrt{\frac{(1-ct)v_f}{a}}$  represents local Reynolds number.

### Entropy analysis

Entropy generation rate is [32]:

$$S_G = S_H(\text{entropy via heat transfer}) + S_F(\text{entropy via fluid friction}). \tag{17}$$

Or

$$\begin{aligned} S_G = \frac{k_{nf}}{T_h^2} \left( \left( \frac{\partial T}{\partial x} \right)^2 + \left( \frac{\partial T}{\partial y} \right)^2 \right) \\ + \frac{\mu_{nf}}{T_h} \left( 4 \left( \frac{\partial u}{\partial x} \right)^2 + \left( \frac{\partial v}{\partial x} + \frac{\partial u}{\partial y} \right)^2 \right). \end{aligned} \tag{18}$$

Non-dimensional entropy generation is

$$Ns = N_H(\text{entropy via heat transfer}) + N_F(\text{entropy via fluid friction}), \tag{19}$$

$$Ns = \frac{S_G}{S_{G_0}} = \theta^2 + \frac{Pr}{\Omega(k_{nf}/k_f)(1-\phi)^{2.5}}(4Ec_f'^2 + Ec_{1f}'^2) \tag{20}$$

where  $S_{G_0} = \frac{k_{nf}(T_m - T_h)}{T_h^2 h^2}$ . (21)

Bejan number is [32]:

$$Be = \frac{N_H(\text{entropy via heat transfer})}{N_G(\text{Total entropy})}, \tag{22}$$

$$Be = \frac{\theta^2}{\theta^2 + \frac{Pr}{\Omega(k_{nf}/k_f)(1-\phi)^{2.5}}(4Ec_f'^2 + Ec_{1f}'^2)}. \tag{23}$$

Note that Bejan number ( $Be$ ) lies between 0 and 1.  $N_H$  dominates over  $N_F$  when  $0.5 < Be \leq 1.0$ , and  $N_F$  overrides  $N_H$  for  $0 \leq Be < 0.5$ , while for  $Be = 1.0$  both  $N_H$  and  $N_F$  are equal.

### Solution via shooting method

Governing equations for flow are solved via shooting method using the fifth-order Runge–Kutta algorithm (bvp4c). First, we have an interest to write the first-order initial value problem as follows [4, 38, 41, 42]:

$$f = s_1, \tag{24}$$

$$f' = s_2, \tag{25}$$

$$f'' = s_3, \tag{26}$$

$$f''' = s_4, \tag{27}$$

$$s_4' = f^{(iv)} = (1-\phi)^{2.5} \left( 1 - \phi + \phi \frac{\rho_{CNT}}{\rho_f} \right) \left( \frac{Sq}{2} (\eta s_4 + 3s_3) - s_2 s_3 + s_1 s_4 \right), \tag{28}$$

$$\theta = s_5, \tag{29}$$

$$\theta' = s_6, \tag{30}$$

$$s_6' = \frac{\left( 1 - \phi + \phi \frac{(\rho_{cp})_{CNT}}{(\rho_{cp})_f} \right)}{\left( (k_{nf}/k_f) \right)} \left( -Pr(s_1 s_6 - \frac{Sq}{2} \eta s_6) \right) - \frac{Pr}{(1-\phi)^{2.5}} (Ec_1 s_3^2 + 4Ec_s s_2^2). \tag{31}$$

along with

$$\begin{aligned} s_2(0) &= 1, \\ \left( \frac{k_{nf}}{k_f} \right) Ms_6(0) + Pr \left( 1 - \phi + \phi \frac{\rho_{CNT}}{\rho_f} \right) s_1(0) &= 0, \\ s_5(0) &= 0, \\ s_2(1) = 1, \quad s_1(1) = 1, \quad s_5'(1) &= 1. \end{aligned} \tag{32}$$

## Analysis

### Analysis for flow and temperature

In this subsection, influences of involved parameters on flow and temperature are analyzed graphically. Figures 1–3 are plotted in order to study variations of flow under  $Sq$ ,  $\phi$  and  $M$ . Intensification in flow is seen for larger  $Sq$ . Variation in flow via  $Sq$  can be studied in two cases: (1)  $Sq > 0$ , (2)  $Sq < 0$ . Here,  $Sq > 0$  is associated with motion of the squeezing plate (upper plate) toward stretchable plate (lower plate), while  $Sq < 0$  corresponds to motion of the squeezing plate (upper plate) away from stretchable plate (lower plate). For higher  $Sq$  ( $Sq > 0$ ), the velocity of fluid increases due to influence of a force (squeezing force) felt by fluid particles. Also the increments in  $\phi$  and  $M$  lead to an enhancement in flow. Physically, an increment in  $M$  is associated with more rapid flow of heated fluid toward melting surface which intensifies flow. Interestingly, single-walled CNTs show overriding trends when compared with multiple-walled CNTs. Variations in temperature via  $Sq$ ,  $\phi$  and  $M$  are labeled in Figs. 4–6. Reduction in temperature is observed for an increment in  $Sq$  ( $Sq > 0$ ).

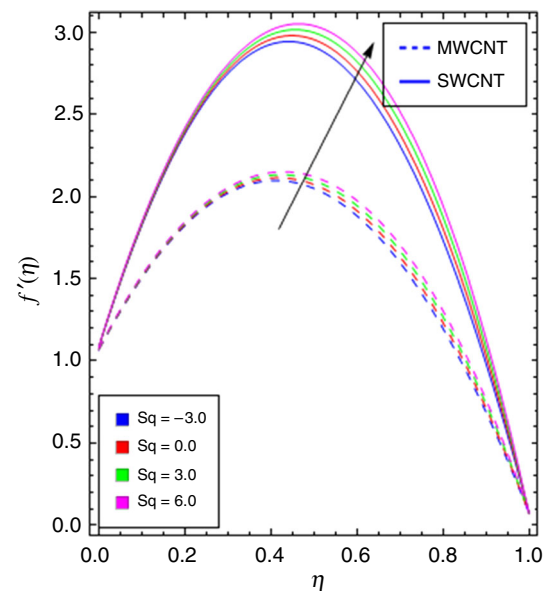


Fig. 1  $f'(\eta)$  via  $Sq$

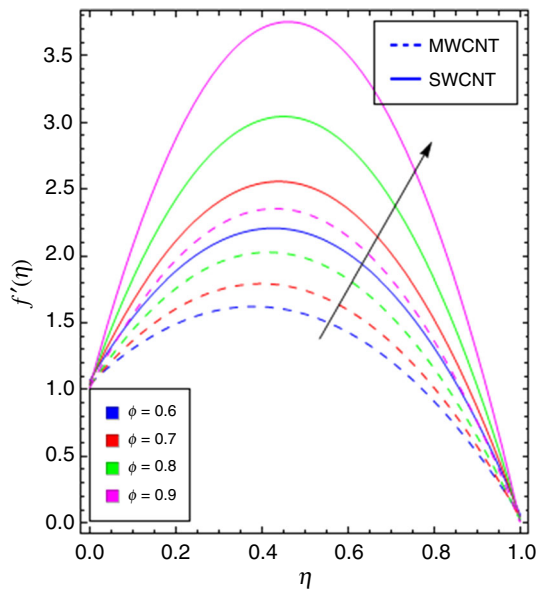


Fig. 2  $f'(\eta)$  via  $\phi$

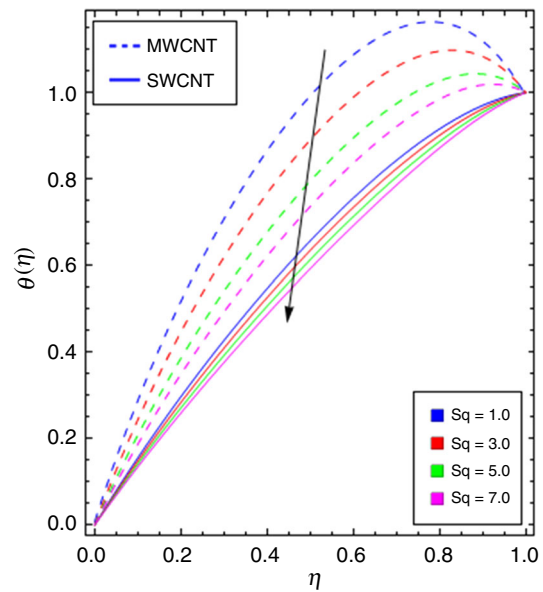


Fig. 4  $\theta(\eta)$  via  $Sq$

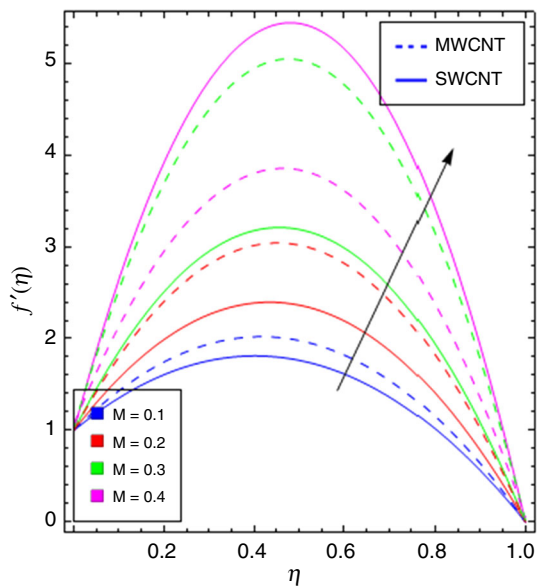


Fig. 3  $f'(\eta)$  via  $M$

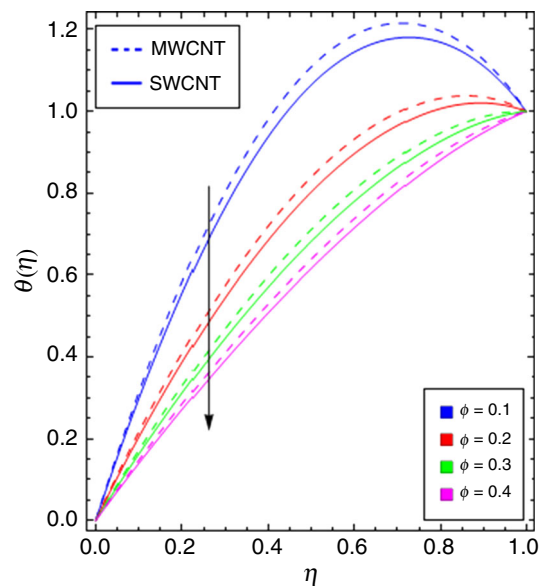
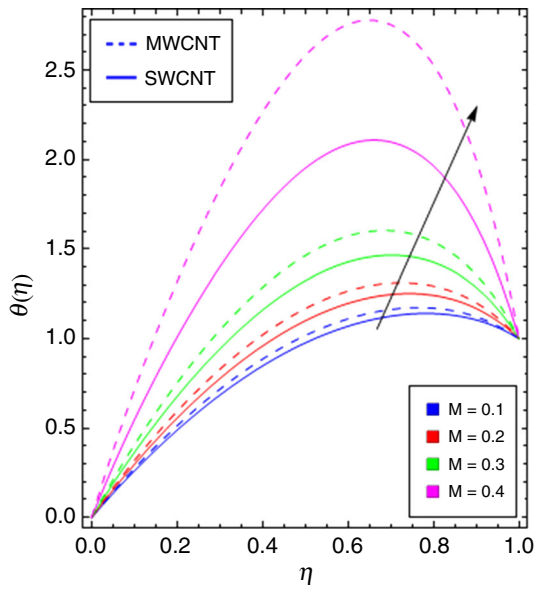
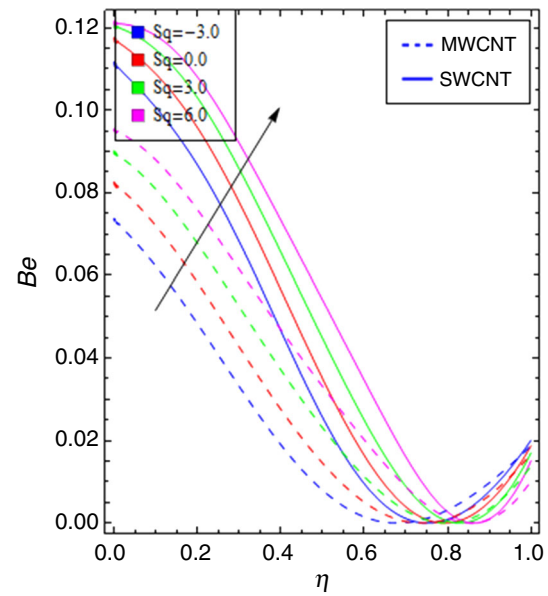
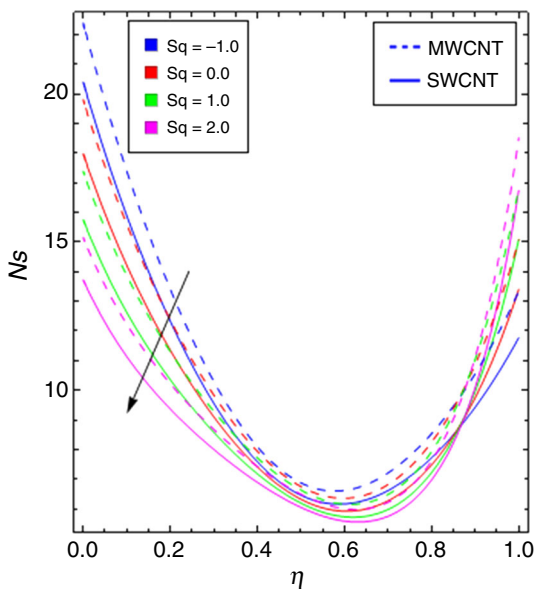
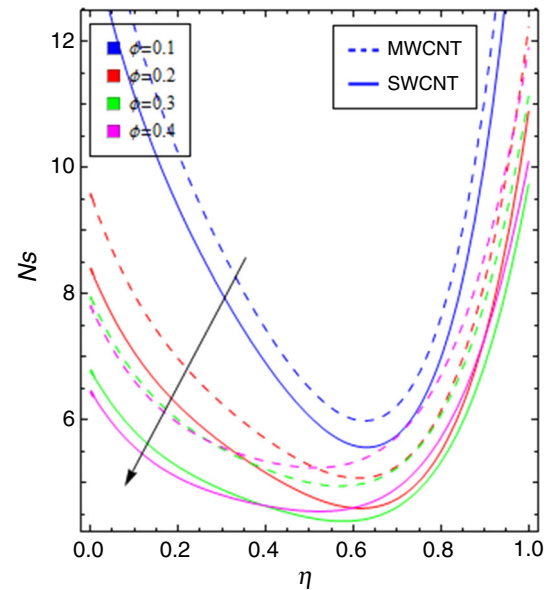


Fig. 5  $\theta(\eta)$  via  $\phi$

Higher  $Sq$  leads to small collision among the fluid particles. Hence, temperature decays while the associated penetration depth rises. Decay in temperature is noted with the variations in  $\phi$  and  $M$ , while opposite trend is seen for associated penetration depth. Physically, higher  $M$  leads to more flow from hot fluid toward the melting surface. Hence, fluid temperature decays. Furthermore, overriding impact is observed for single-walled CNTs.

### Analysis for entropy generation and Bejan number

Variations in  $N_s$  and  $Be$  via  $Sq$ ,  $\phi$  and  $M$  are depicted in this subsection. Figures 7, 9 and 11 illustrate variations in  $N_s$  via  $Sq$ ,  $\phi$  and  $M$ , respectively. It is noticed that  $N_s$  reduces with an increment in  $Sq$ . Furthermore, production of entropy is maximum at the both walls, while it is minimum at the center of channel. Higher  $\phi$  leads to smaller  $N_s$ , while  $N_s$  intensifies for larger  $M$ . At both walls, production of entropy is maximum, while at center, the entropy production is minimum. Further, single-walled

Fig. 6  $\theta(\eta)$  via  $M$ Fig. 8  $Be$  via  $Sq$ Fig. 7  $Be$  via  $Sq$ Fig. 9  $Ns$  via  $\phi$ 

CNTs show overriding trend comparatively with multiple-walled CNTs. In order to analyze the dominance of entropy due to fluid friction over entropy due to heat transfer or vice versa,  $Be$  is labeled via  $\eta$  in Figs. 8, 10 and 12. Intensification in  $Be$  is noted with an increment in  $Sq$ . It is observed that at the lower wall the entropy due to fluid friction is prominent for higher  $Sq$ . Reduction in  $Be$  is noted for higher  $\phi$ . It is also observed that entropy via fluid friction shows overriding behavior at both walls.  $Be$  decays with an increment in  $M$ , and dominance in entropy via fluid

friction is noticed at both walls over entropy via heat transfer. Furthermore, single-walled CNTs show prominent behavior (Figs. 9–12).

Table 1 presents constructed thermophysical features of nanoparticles and base liquid, while numerical values of  $C_f$  and  $Nu_x$  under  $Sq$ ,  $\phi$  and  $M$  are presented in Tables 2 and 3.

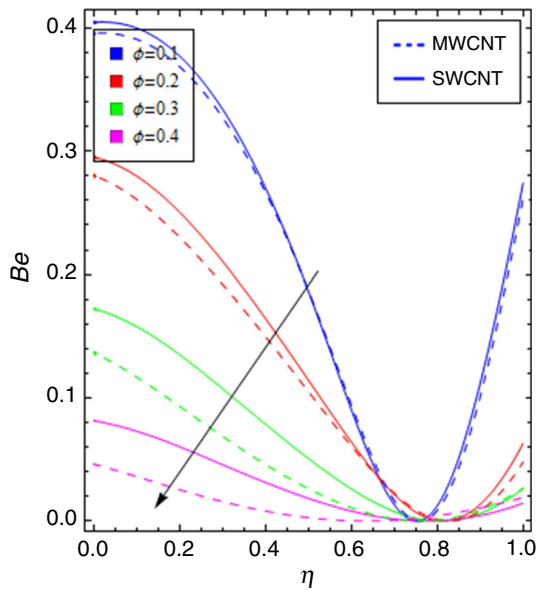


Fig. 10  $Be$  via  $\phi$

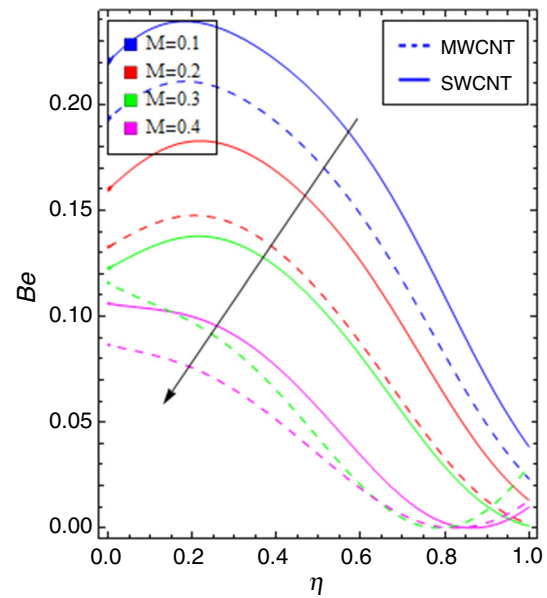


Fig. 12  $Be$  via  $M$

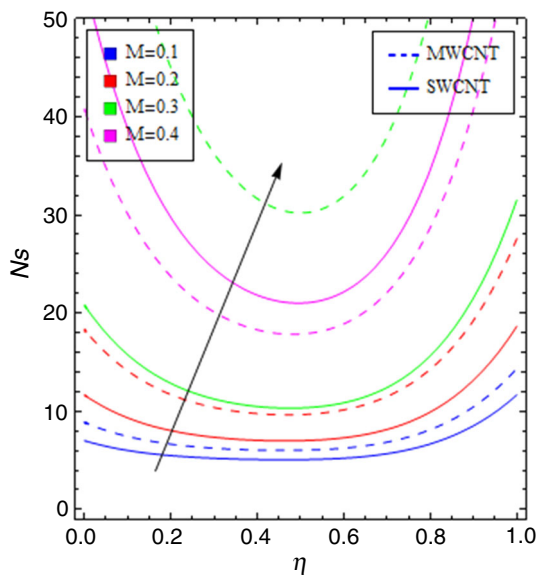


Fig. 11  $Ns$  via  $M$

**Final remarks**

The key points of the presented analysis are

- Intensification in flow is observed with the increment in  $Sq$ ,  $\phi$  and  $M$ .
- Decay in temperature is noted against  $Sq$ ,  $\phi$  and  $M$ .
- Single-walled CNTs show overriding behavior than multiple-walled CNTs in terms of both flow and temperature.
- Intensification in heat transfer rate is analyzed for larger  $Sq$ ,  $\phi$  and  $M$ .

**Table 1** Thermophysical features of base liquid and CNTs [40]

| Physical features                    | Base liquid | Physical features |       |
|--------------------------------------|-------------|-------------------|-------|
|                                      | Water       | SWCNT             | MWCNT |
| $\rho/\text{kg m}^{-3}$              | 997         | 2600              | 1600  |
| $c_p/\text{J kg}^{-1} \text{K}^{-1}$ | 4179        | 425               | 796   |
| $k/\text{W m}^{-1} \text{K}^{-1}$    | 0.613       | 6600              | 3000  |

**Table 2** Analysis of  $C_f$  via  $Sq$ ,  $\phi$  and  $M$

| $Sq$  | $\phi$ | $M$ | $C_f(\text{SWCNTs})$ | $C_f(\text{MWCNTs})$ |
|-------|--------|-----|----------------------|----------------------|
| - 1.0 | 0.5    | 0.7 | 82.5                 | 49.3                 |
|       |        |     | 82.8                 | 49.4                 |
|       |        |     | 83.1                 | 49.5                 |
|       |        |     | 83.5                 | 49.6                 |
|       |        |     | 83.8                 | 49.8                 |
| 1.0   | 0.1    | 0.7 | 6.8                  | 6.2                  |
|       |        |     | 7.8                  | 6.3                  |
|       |        |     | 11.8                 | 8.4                  |
|       |        |     | 20.3                 | 13.2                 |
|       |        |     | 38.6                 | 23.9                 |
| 1.0   | 0.1    | 0.1 | 3.6                  | 3.7                  |
|       |        | 0.2 | 4.9                  | 5.1                  |
|       |        | 0.3 | 6.8                  | 7.4                  |
|       |        | 0.4 | 11.5                 | 14.8                 |
|       |        | 0.5 | 25.7                 | 29.4                 |

**Table 3** Analysis of  $Nu_x$  via  $Sq, \phi$  and  $M$  when  $Ec = Ec_1 = 0.2$ .

| $Sq$  | $\phi$ | $M$ | $Nu_x$ (SWCNTs) | $Nu_x$ (MWCNTs) |
|-------|--------|-----|-----------------|-----------------|
| – 1.0 | 0.5    | 0.7 | 24.3            | 9.7             |
| 0.0   |        |     | 24.5            | 9.8             |
| 1.0   |        |     | 24.7            | 9.9             |
| 2.0   |        |     | 24.9            | 10.0            |
| 3.0   |        |     | 25.1            | 10.1            |
| 1.0   | 0.1    | 0.7 | 11.4            | 9.3             |
|       | 0.2    |     | 12.0            | 9.4             |
|       | 0.3    |     | 14.0            | 9.5             |
|       | 0.4    |     | 16.5            | 9.6             |
|       | 0.5    |     | 19.2            | 9.7             |
| 1.0   | 0.1    | 0.1 | 7.0             | 7.4             |
|       |        | 0.2 | 9.6             | 10.3            |
|       |        | 0.3 | 12.7            | 13.9            |
|       |        | 0.4 | 16.7            | 18.7            |
|       |        | 0.5 | 21.9            | 29.9            |

- Entropy production rate decays with an increment in  $Sq$  and  $\phi$ .
- Bejan number is an increasing function of  $Sq$ , while it reduces for  $\phi$  and  $M$ .
- Role of multiple-walled CNTs is prominent than single-walled CNTs for both entropy generation and Bejan number.

## References

- Choi SUS, Eastman JA. Enhancing thermal conductivity of fluids with nanoparticles. In: The proceedings of the 1995 ASME. International mechanical engineering congress and exposition, San Francisco: ASME, FED 231/MD; 1999. Vol. 66, pp. 99–105.
- Hayat T, Muhammad K, Alsaedi A, Farooq M. Features of Darcy-Forchheimer flow of carbon nanofluid in frame of chemical species with numerical significance. *J Cent South Univ*. 2019;26:1260–70.
- Rae B, Shahraki F, Jamailahmadi M, Peyghambarzede SM. Experimental study on the heat transfer and flow properties of  $\gamma$ -Al<sub>2</sub>O<sub>3</sub>/water nanofluid in a double-tube heat exchanger. *J Therm Anal Calorim*. 2017;127:2561–75.
- Hayat T, Ahmed B, Abbasi FM, Alsaedi A. Numerical investigation for peristaltic flow of Carreau-Yasuda magneto-nanofluid with modified Darcy and radiation. *J Therm Anal Calorim*. 2019;12:1–9.
- Khan MI, Muhammad K, Hayat T, Farooq S, Alsaedi A. Numerical treatment for Darcy-Forchheimer flow of carbon nanotubes due to convectively heat nonlinear curved stretching surface. *Int J Numer Methods Heat & Fluid Flow*. 2019. <https://doi.org/10.1108/HFF-01-2019-0016>.
- Hayat T, Muhammad K, Muhammad T, Alsaedi A. Melting heat in radiative flow of carbon nanotubes with homogeneous-heterogeneous reactions. *Commun Theor Phys*. 2018;69:441–8.
- Dinarvand S, Pop I. Free-convective flow of copper/water nanofluid about a rotating down-pointing cone using Tiwari-Das nanofluid scheme. *Adv Powder Technol*. 2017;28:900–9.
- Muhammad K, Hayat T, Alsaedi A. Squeezed flow of Jeffrey nanomaterial with convective heat and mass conditions. *Phys Scr*. 2019. <https://doi.org/10.1088/1402-4896/ab234f>.
- Soltani S, Kasaiean A, Sarrafha H, Wen D. An experimental investigation of a hybrid photovoltaic/thermoelectric system with nanofluid application. *Sol Energy*. 2017;155:1033–43.
- Hayat T, Muhammad K, Alsaedi A, Asghar S. Numerical study for melting heat transfer and homogeneous-heterogeneous reactions in flow involving carbon nanotubes. *Results Phys*. 2018;8:415–21.
- Ullah I, Waqas M, Hayat T, Alsaedi A, Khan MI. Thermally radiated squeezed flow of magneto-nanofluid between two parallel disks with chemical reaction. *J Therm Anal Calorim*. 2018;135:1021–30.
- Hayat T, Muhammad K, Farooq M, Alsaedi A. Unsteady squeezing flow of carbon nanotubes with convective boundary conditions. *PLoS ONE*. 2016;11:0152923.
- Mahian O, Kolsi L, Amani M, Estellé P, Ahmadi G, Kleinstreuer C, Marshall JS, Siavashi M, Taylor RA, Niazmand H, Wongwises S, Hayat T, Kolanjiyil A, Kasaiean A, Pop I. Recent advances in modeling and simulation of nanofluid flows-Part I: fundamentals and theory. *Phys Rep*. 2018. <https://doi.org/10.1016/j.physrep.2018.11.004>.
- Hayat T, Muhammad K, Alsaedi A. Melting effect in MHD stagnation point flow of Jeffrey nanomaterial. *Phys Scr*. 2019. <https://doi.org/10.1088/1402-4896/ab210e>.
- Mahian O, Kolsi L, Amani M, Estellé P, Ahmadi G, Kleinstreuer C, Marshall JS, Taylor RA, Abu-Nada E, Rashidi S, Niazmand H, Wongwises S, Hayat T, Kasaiean A, Pop I. Recent advances in modeling and simulation of nanofluid flows-Part II: applications. *Phys Rep*. 2018. <https://doi.org/10.1016/j.physrep.2018.11.003>.
- Hayat T, Muhammad K, Ullah I, Alsaedi A, Asghar S. Rotating squeezed flow with carbon nanotubes and melting heat. *Phys Scr*. 2018. <https://doi.org/10.1088/1402-4896/aaef66>.
- Majka TM, Raftopoulos KN, Pielichowski K. The influence of POSS nanoparticles on selected thermal properties of polyurethane-based hybrids. *J Therm Anal Calorim*. 2018;133:289–301.
- Hayat T, Aziz A, Muhammad T, Alsaedi A. Numerical simulation for Darcy-Forchheimer three-dimensional rotating flow of nanofluid with prescribed heat and mass flux conditions. *J Therm Anal Calorim*. 2019;136:2087–95.
- Hayat T, Aziz A, Muhammad T, Alsaedi A. Effects of binary chemical reaction and Arrhenius activation energy in Darcy-Forchheimer three-dimensional flow of nanofluid subject to rotating frame. *J Therm Anal Calorim*. 2019;136:1769–79.
- Bejan A. *Advanced engineering thermodynamics*. Hoboken: Wiley; 2006.
- Bejan A. A study of entropy generation in fundamental convective heat transfer. *ASME J Heat Transf*. 1979;101:718–25.
- Bejan A. The thermodynamic design of heat and mass transfer processes and devices. *Int J Heat Fluid Flow*. 1987;8:258–76.
- Lotfi A, Lakzian E. Entropy generation analysis for film boiling: a simple model of quenching. *Eur Phys J Plus*. 2016;131:1–10.
- Rashidi S, Akar S, Bovand M, Ellahi R. Volume of fluid model to simulate the nanofluid flow and entropy generation in a single slope solar still. *Renew Energy*. 2018;115:400–10.
- Shehzad N, Zeeshan A, Ellahi R, Rashidi S. Modelling study on internal energy loss due to entropy generation for non-Darcy poiseuille flow of silver-water Nanofluid: an application of purification. *Entropy*. 2018;20:851. <https://doi.org/10.3390/e20110851>.



26. Soltanmohammadi R, Lakzian E. Improved design of wells turbine for wave energy conversion using entropy generation. *Meccanica*. 2016;51:1713–22.
27. Lakzian E, Soltanmohammadi R, Nazeryan M. A comparison between entropy generation analysis and first law efficiency in a monoplane wells turbine. *Scientia Iranica B*. 2016;23:2673–81.
28. Zhu L, Yu J. Optimization of heat sink of thermoelectric cooler using entropy generation analysis. *Int J Therm Sci*. 2017;118:168–75.
29. Heshmatian S, Bahiraei M. Numerical investigation of entropy generation to predict irreversibilities in nanofluid flow within a microchannel: effects of Brownian diffusion, shear rate and viscosity gradient. *Chem Eng Sci*. 2017;172:52–65.
30. Sheikholeslami M, Ellahi R, Shafee A, Li Z. Numerical investigation for second law analysis of ferrofluid inside a porous semi annulus: an application of entropy generation and exergy loss. *Int J Numer Meth Heat Fluid Flow*. 2019;29:1079–102.
31. Zeeshan A, Shehzad N, Abbas T, Ellahi R. Effects of radiative electro-magnetohydrodynamics diminishing internal energy of pressure-driven flow of titanium dioxide-water nanofluid due to entropy generation. *Entropy*. 2019;21:1–25.
32. Khan MI, Hayat T, Waqas M, Khan MI, Alsaedi A. Entropy generation minimization (EGM) in nonlinear mixed convective flow of nanomaterial with Joule heating and slip condition. *J Mol Liq*. 2018;256:108–20.
33. Rahman RGA, Khadar MM, Megahed AM. Melting phenomenon in magnetohydrodynamics steady flow and heat transfer over a moving surface in the presence of thermal radiation. *Chin Phys B*. 2013;22:030202.
34. Hayat T, Bashir G, Waqas M, Alsaedi A, Ayub M, Asghar S. Stagnation point flow of nanomaterial towards nonlinear stretching surface with melting heat. *Neural Comput Appl*. 2016. <https://doi.org/10.1007/s00521-016-2704-y>.
35. Sheikholeslami M, Rokni HB. Melting heat transfer influence on nanofluid flow inside a cavity in existence of magnetic field. *Int J Heat Mass Transf*. 2017;114:517–26.
36. Hayat T, Muhammad K, Farooq M, Alsaedi A. Melting heat transfer in stagnation point flow of carbon nanotubes towards variable thickness surface. *AIP Adv*. 2016;6:015214.
37. Khan WA, Khan M, Irfan M, Alshomrani AS. Impact of melting heat transfer and nonlinear radiative heat flux mechanisms for the generalized Burgers fluids. *Results Phys*. 2017;7:4025–32.
38. Hayat T, Muhammad K, Alsaedi A, Ahmad B. Melting effect in squeezing flow of third-grade fluid with non-Fourier heat flux model. *Phys Scr*. 2019. <https://doi.org/10.1088/1402-4896/ab1c2c>.
39. Soomro FA, Usman M, Haq RU, Wang W. Melting heat transfer analysis of Sisko fluid over a moving surface with nonlinear thermal radiation via collocation method. *Int J Heat Mass Transf*. 2018;126:1034–42.
40. Xue Q. Model for thermal conductivity of carbon nanotube based composites. *Phys B Condense Matter*. 2005;368:302–7.
41. Hayat T, Muhammad K, Khan MI, Alsaedi A. Theoretical investigation of chemically reactive flow of water-based carbon nanotubes (single-walled and multiple walled) with melting heat transfer. *Pramana J Phys*. 2019. <https://doi.org/10.1007/s12043-019-1722-6>.
42. Muhammad K, Hayat T, Alsaedi A, Asghar S. Stagnation point flow of basefluid (gasoline oil), nanomaterial (CNTs) and hybrid nanomaterial (CNTs + CuO): a comparative study. *Mater Res Express*. 2019;6(10):105003.

**Publisher's Note** Springer Nature remains neutral with regard to jurisdictional claims in published maps and institutional affiliations.